Zn(II), Cd(II) and Pb(II) complexation with pyridinecarboxylate containing ligands†

Raquel Ferreirós-Martínez, David Esteban-Gómez, Carlos Platas-Iglesias, Andrés de Blas and Teresa Rodríguez-Blas

Departamento de Química Fundamental, Universidade da Coruña, Campus da Zapateira s/n, Coruña, Spain

Dalton Transactions Issue 42, pages 5754–5765, 14 November 2008
Received 22 May 2008, Accepted 03 July 2008, First published 09 September 2008

How to cite:
Zn(II), Cd(II) and Pb(II) complexation with pyridinecarboxylate containing ligands. R. Ferreirós-Martínez, D. Esteban-Gómez, C. Platas-Iglesias, A. de Blas and T. Rodríguez-Blas, *Dalt. Trans.*, 2008, 5754–5765. DOI: 10.1039/B808631A.

Abstract

Herein, we report the coordination properties towards Zn(II), Cd(II) and Pb(II) of two hexadentate ligands containing pyridinecarboxylate groups with ethane-1,2-diamine (bcpe) or cyclohexane-1,2-diamine (bcpc) backbones. The X-ray crystal structures of [Zn(bcpe)], [Cd(bcpe)] and [Cd(bcpc)] show hexadentate binding of the ligand to the metal ions, with the coordination polyhedron being best described as a severely distorted octahedron. The X-ray crystal structure of the Pb(II) analogue shows the presence of tetrameric structural units $[Pb_4(bcpe)_4]$ in which the four Pb(II) ions are bridged by carboxylate oxygen atoms. While in the Zn(II) and Cd(II) complexes the bcpe ligand adopts a twist–wrap (tw) conformation in which the ligand wraps around the metal ion by twisting the pyridyl units relative to each other, for the Pb(II) complex a twist–fold (tf) conformation, where a slight twisting of the pyridyl units is accompanied by an overall folding of the two pyridine units relative to each other is observed. Theoretical calculations performed at the DFT (B3LYP) level on the [Pb(bcpe)] and [Pb(bcpc)] systems indicate that the tf conformation is more stable than the tw form both in the solid state and in aqueous solution. The analysis of the natural bond orbitals (NBOs) indicate that the Pb(II) lone-pair is polarized by a substantial 6p contribution, which results in a hemi-directed coordination geometry around the metal ion. Potentiometric studies have been carried out to determine the protonation constants of the ligands and the stability constants of the complexes with Zn(II), Cd(II), Pb(II) and Ca(II). The replacement of the ethylene backbone of bcpe by a cyclohexylene ring causes a very important increase in the stability constant of the Pb(II) complex (*ca.* 2.3 log*K* units), while this effect is less important for Cd(II) (*ca.* 1.4 log*K* units). However, the introduction of the cyclohexylene ring does not substantially affect the stability of the Zn(II) and Ca(II) complexes. The ligand bcpc shows Pb/Ca and Cd/Ca selectivities [$10^{8.9}$ and $10^{9.8}$, respectively] superior to those of extracting agents, such as EDTA, already used in Pb(II) and Cd(II) removal from contaminated water and soils.

Keywords: picolinate ligands; crystal structures; DFT calculations; lone-pair activity; heavy-metal complexes

Introduction

The interest in the coordination chemistry of cadmium and lead is related not only to the widespread industrial uses of their compounds, but also to their inherent toxicity and health effects.[1,2] Mostly, lead poisoning results from an exposure to divalent or inorganic lead, Pb(II), either from inhalation or ingestion.

Once ingested, through the gastrointestinal tract, lead accumulates in soft tissues including vital organs such as the liver, the kidneys or the brain, where it binds to thiol and phosphate groups in nucleic acids, proteins and cell membranes[3–9] resulting in severe neurological and/or haematological effects.[10–13] It also distributes itself within the bones and the teeth, where it may occupy calcium sites in hydroxyapatite. Lead poisoning particularly affects young children who can absorb up to 50% of ingested lead.[11] Recent studies suggest that the developmental toxicity associated with childhood lead poisoning may be attributable to interactions of lead(II) with proteins containing thiol-rich structural zinc binding sites. In the case of structural zinc binding protein sites, the observation that lead binds in a geometry that is fundamentally different from the natural coordination of zinc in these sites, explains why lead disrupts the structure of these peptides and thus, provides the first detailed molecular understanding of the developmental toxicity of lead.[9] Damage to the lungs in cadmium exposed workers was the first human health effect related to cadmium in a report published already in the 1930's.[14] Exposure to Cd(II) causes bone diseases, gastrointestinal and renal dysfunction, and cadmium and cadmium compounds are regarded as carcinogenic to humans.

The removal of toxic heavy metal contaminants from aqueous waste streams is currently an environmental issue of great importance. Precipitation, activated carbon absorption, bioremediation, reverse osmosis, electrolysis, cementation, irradiation, zeolite absorption, evaporation, membrane processes or ion flotation are some of the treatment methods used for heavy metal-containing waste remediation.[15]Solvent extraction and treatment with cation exchange resins are also important, especially if selective extractions are required and/or low concentrations of the target metal ion are present in solution. Solvent extraction occurs when a metal ion associates itself with an organic complexing agent to form a species that is transferred from the aqueous to the organic phase in a two phase system, whereas cation exchange resins are formed by a polymeric skeleton functionalized with a complexing agent capable of binding to the desired metal ion; therefore, these two methods require the presence of a selective complexing agent.

The lack of predictability associated with the coordination chemistry of Pb(II) has been attributed to the interplay of electrostatic factors and ligand constraints that might permit the stereochemical activity of the Pb(II) lone pair. Glusker *et al.*[16]investigated the close relation between the role of the lone pair of Pb(II) and the coordination geometry for a large number of Pb(II) complexes. They found two general structural categories of Pb(II) compounds: holo-directed and hemi-directed, which are distinguished by the disposition of the ligands around the metal ion. In the hemi-directed form the disposition of the ligand(s) donor atom generates a void that is not found in the holo-directed geometry. Complexes with high coordination numbers (9–10) usually adopt holo-directed geometries, while lead(II) complexes with coordination numbers lower than 6 are normally hemi-directed and have a stereochemically active lone pair. Both types of structures are found for the intermediate coordination numbers (6–8). In this case, the stereochemical activity of the lone pair, and hence the geometry, seems to strongly depend on the nature of the donor atoms and the steric repulsion of the ligands. It has been stated that for electronegative donor atoms such as oxygen or nitrogen, hemi-directed structures are energetically favoured.

In this paper, we report two ligands containing pyridinecarboxylate chelating groups (H_2bcpe and H_2bcpc; Scheme 1) designed for Zn(II), Cd(II) and Pb(II) complexation in aqueous solution. It has been recently reported that tripodal and dipodal ligands containing pyridinecarboxylate groups form stable Pb(II) complexes in aqueous solution showing an important selectivity for Pb(II) over Ca(II).[17] A comparative study of the complexes of bcpe and bcpc allows for the assessment of how small structural modifications affect the stability and the structure of the complexes. In particular, one can expect the introduction of the cyclohexyl unit in the ligand skeleton to modulate the rigidity of the inner sphere, which may have consequences on the stability of the complexes.[18] Thermodynamic stability constants of the Zn(II), Cd(II) and Pb(II) complexes of these ligands have been determined by pH potentiometry titrations. The structure of the complexes in solution has been studied by ^{1}H and ^{13}C NMR techniques in D_2O solution. The X-ray crystal structures of the Zn(II), Cd(II) and Pb(II) complexes of bcpe and the Cd(II) complex of bcpc are also

reported. To understand the structural features and electronic properties related to the stereochemical activity of the lead(II) lone pair, the [Pb(L)] systems (L = bcpe or bcpc) have also been characterized by means of DFT calculations (B3LYP model).

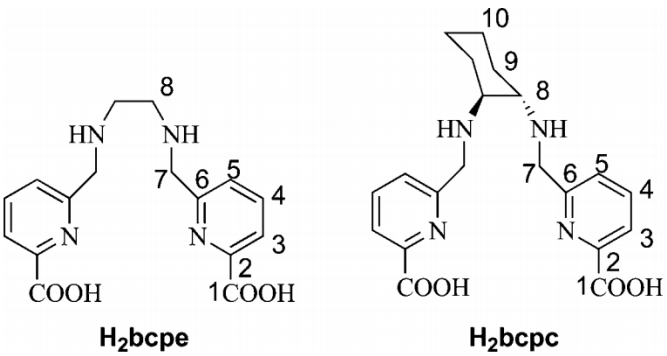

Scheme 1

Results and discussion

Synthesis and X-ray crystal structures

The ligands H_2bcpe and H_2bcpc were obtained in three steps from methyl-6-formylpyridine-2-carboxylate (see Scheme 2). The latter can be obtained from the commercially available pyridine-2,6-dicarboxylic acid in three steps involving the partial reduction of dimethyl pyridine-2,6-dicarboxylate followed by oxidation with SeO_2 (67% overall isolated yield).[19,20]Methyl-6-formylpyridine-2-carboxylate was reacted with ethane-1,2-diamine or (1*R*,2*R*)-diaminecyclohexane to give the Schiff bases**1a** and **1b** in 80–90% yield. Compounds **1a** and **1b** were reduced with sodium tetrahydroborate, affording the amines **2a** and**2b** in excellent yield (*ca.* 90%). The desired ligands were prepared in 20–40% isolated yield by hydrolysis of the methylester groups in 6 M HCl. H_2bcpe and H_2bcpc were obtained in *ca.* 20% overall yields as calculated from the commercially availablepyridine-2,6-dicarboxylic acid.

The structure of the protonated ligand H_2bcpe·2HCl was determined by X-ray diffraction analysis (Fig. 1). The ligandcrystallizes in the centrosymmetric $P2_1/c$ monoclinic space group, and the asymmetric unit comprises of half a molecule. The crystals contain a $[H_4bcpe]^{2+}$ cation and two chloride anions. The conformation of the ligand is such that the two protonated amine nitrogen atoms are as far apart as possible from each other to keep the electrostatic repulsion to a minimum. The conformation of the ligand is also conditioned by intermolecular hydrogen bonding interactions between the protonated amine and carboxylic acid groups and chloride anions [N2···Cl1 3.1244(14) Å, N2···H2A 0.90 Å, Cl1···H2A 2.29 Å, N2–H2A–Cl1 159.9°; O2···Cl1 3.1327(15) Å, O2···H2 0.82 Å, Cl1···H2 2.51 Å, O2–H2–Cl1 134.1°]. Intramolecular hydrogen bonding interactions also exist between the protonated carboxylic acid group and the pyridine nitrogen atoms: [O2···N1 2.644(2) Å, O2···H2 0.82 Å, N1···H2 2.15 Å, O2–H2–N1 118.7°].

Compounds of the general formula $[M(bcpe)]\cdot nH_2O$ (M = Zn or Cd; n = 2 or 3) can be easily prepared by the reaction between H_2bcpe·2HCl and the corresponding metal perchlorate in the presence of four equivalents of triethylamine. The low solubility of $PbCl_2$ prevents the preparation of the analogous Pb(II) complex by using H_2bcpe·2HCl. Thus, the latter compound was reacted with $Ag(NO_3)$ to give $H_2bcpe\cdot 2HNO_3$ in 82% yield. The subsequent reaction of $H_2bcpe\cdot 2HNO_3$, with lead nitrate in the presence of triethylamine, gave the desired Pb(II) complex $[Pb(bcpe)]\cdot 2H_2O$. The IR spectra of the three complexes (KBr discs) show two bands at *ca.* 1620 and 1380 cm^{-1} corresponding to the asymmetric and symmetric stretching modes of the coordinated carboxylate groups, respectively. Moreover, the IR spectrum of the Pb complex does not show

bands associated with the NO_3^- group, in agreement with the above given formulation. The FAB mass spectra of the three complexes display intense peaks due to $[M(L + H)]^+$ (M = Zn, Cd or Pb), which confirms the formation of the desired complexes.

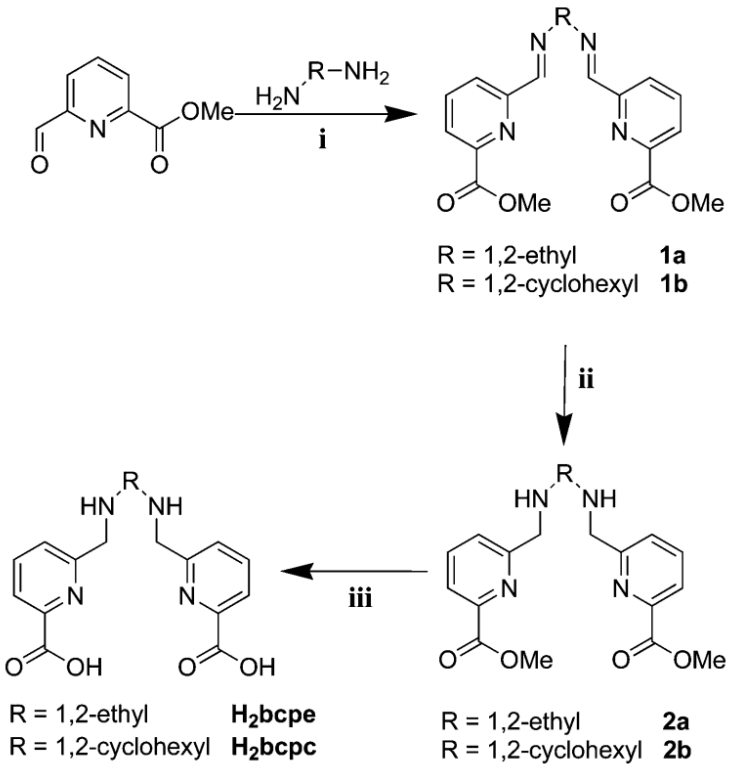

Scheme 2. (i) MeOH, reflux, (ii) MeOH, $NaBH_4$, (iii) 6M HCl, reflux.

The solid state structures of the zinc and cadmium complexes $[Zn(bcpe)]\cdot 3H_2O$ and $[Cd(bcpe)]\cdot 2H_2O$ were determined by single-crystal X-ray diffraction analyses. The crystals contain the expected neutral complexes and non-coordinated water molecules hydrogen bonded to the oxygen atoms of the carboxylate groups. Fig. 2 shows a view of both complexes, and bond lengths and angles of the metal coordination environments are listed in Table 1. In both complexes the metal ion is directly bound to the six donor atoms of the ligand, with the coordination polyhedron around the metal ion being best described as a severely distorted octahedron. A ligand, such as bcpe, can coordinate in an octahedral fashion to a metal ion with three possible geometries: *trans*(O,O), *trans*(N_{py}, N_{py}), and *cis*(O,O) [this one also named as *cis*(N_{py}, N_{py})],[21] where N_{py} denotes a nitrogen atom of a pyridine unit. The X-ray structures of the [Zn(bcpe)] and [Cd(bcpe)] complexes (Fig. 2) show that both complexes adopt *trans*(N_{py}, N_{py}) conformations in the solid state, the N(1)–M(1)–N(4) angles amounting to 172.73(8) and 176.0(2)° for the Zn and Cd complexes, respectively. The two tridentate aminopicolinate moieties bind meridionally through their N-amine, N-pyridine and O-carbonyl atoms. The meridional arrangement of the aminopicolinate moieties can be proven by the dihedral angles that the terminal donor atoms of each aminopicolinate moiety [O(3)–N(3) and O(1)–N(2)] form with the N(1)–N(4) axis. This angle, indicated as τ, has ideal values of 54.7, 90 and 180° for the un-distorted *u-fac*, *s-fac* and *mer* isomers.[22] The large amount of distortion of the octahedral coordination leads to a considerable deviation from the ideal value of 180° (τ = 166.8° for O1N1–N4N2 and τ = 164.2° for O3N4–N1N3 in [Zn(bcpe)] and τ = 171.7° for O1N1–N4N2 and τ = 166.1° for O3N4–N1N3 in [Cd(bcpe)]).

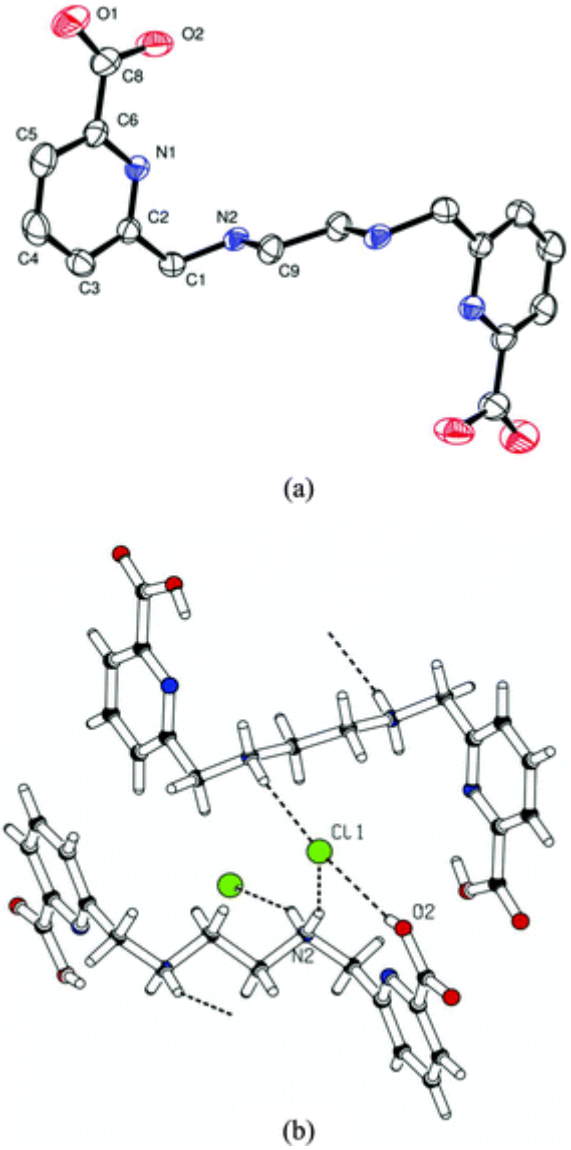

Fig. 1. (a) X-Ray crystal structure of H_2bcpe·2HCl with atom labelling; hydrogen atoms are omitted for simplicity; the ORTEP plot is drawn at the 50% probability level. (b) View of H_2bcpe·2HCl showing the hydrogen bonding interactions.

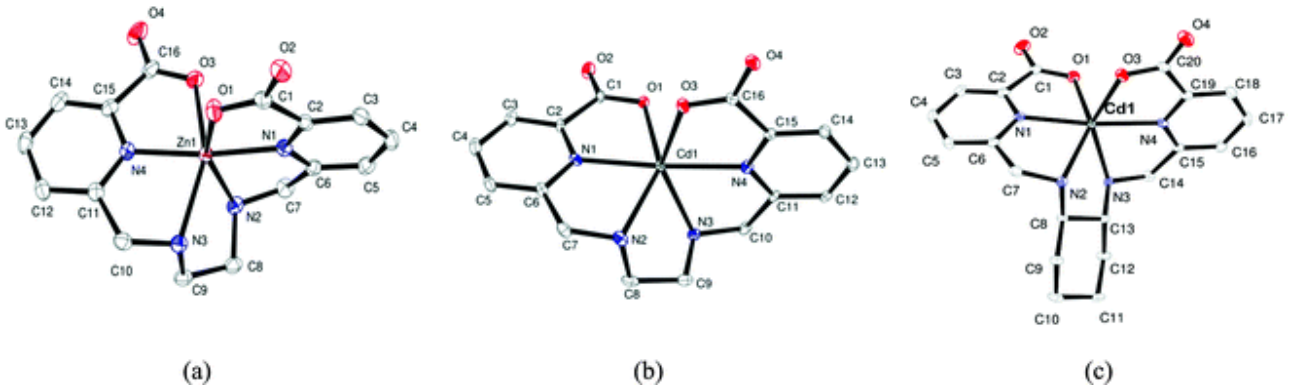

Fig. 2. X-Ray crystal structures of (a) [Zn(bcpe)]·3H_2O, (b) [Cd(bcpe)]·2H_2O and (c) [Cd(bcpc)] with atom labelling; hydrogen atoms and water molecules are omitted for simplicity. The ORTEP plots are drawn at the 50% probability level.

Table 1. Bond lengths (Å) and angles (°) for the Zn(II) and Cd(II) complexes of bcpe and bcpc (see Fig. 2 for numbering scheme).

	[Zn(bcpe)]	[Cd(bcpe)]	[Cd(bcpc)]
M(1)–N(1)	2.052(2)	2.280(4)	2.257(2)
M(1)–N(2)	2.214(2)	2.383(4)	2.372(2)
M(1)–N(3)	2.234(2)	2.370(4)	2.395(2)
M(1)–N(4)	2.054(2)	2.280(4)	2.257(2)
M(1)–O(1)	2.192(2)	2.323(3)	2.327(2)
M(1)–O(3)	2.115(2)	2.317(3)	2.300(2)
N(1)–M(1)–N(4)	172.73(8)	176.0(1)	168.86(7)
N(4)–M(1)–O(3)	78.27(8)	71.3(1)	71.77(7)
N(1)–M(1)–O(3)	98.36(8)	106.0(1)	109.98(7)
N(1)–M(1)–O(1)	76.14(8)	70.8(1)	71.56(7)
N(4)–M(1)–O(1)	97.80(8)	106.2(1)	97.40(7)
O(3)–M(1)–O(1)	97.57(7)	90.6(1)	95.49(7)
N(1)–M(1)–N(2)	76.97(8)	71.7(1)	72.70(7)
N(4)–M(1)–N(2)	109.69(8)	111.6(1)	117.56(7)
O(3)–M(1)–N(2)	96.64(7)	105.8(1)	109.43(7)
O(1)–M(1)–N(2)	151.09(8)	141.9(1)	141.66(7)
N(1)–M(1)–N(3)	109.03(8)	112.7(1)	107.96(7)
N(4)–M(1)–N(3)	75.40(8)	70.6(1)	72.28(7)
O(3)–M(1)–N(3)	151.40(8)	140.1(1)	141.54(7)
O(1)–M(1)–N(3)	96.88(7)	111.1(1)	102.23(7)
N(2)–M(1)–N(3)	82.03(8)	77.9(1)	76.13(7)

The bcpe ligand forms five, five-membered chelate rings imposing large distortions on the ideally octahedral coordination angles. Indeed, while the *trans*N(1)–M(1)–N(4) angles are relatively close to 180°, the *trans* angles O(1)–M(1)–N(2) and O(3)–M(1)–N(3) markedly deviate from linearity (Table 1). This distortion is more important in the Cd(II) complex than in the Zn(II) analogue. The vectors defined by the metal ion and the axial donors N(1) and N(4) form angles with the vectors containing the metal ion and the equatorial donor atoms ranging from 75.40–109.69° for [Zn(bcpe)] and from 70.61–112.68° for [Cd(bcpe)], which shows that the distortion from a regular octahedral geometry of these angles (ideal value 90 °) also increases with metal ion size.[23]

The [Zn(bcpe)] and [Cd(bcpe)] complexes present two different sources of chirality: one arising from the five-membered ring formed by the binding of the ethylene diamino moiety (absolute configuration δ or λ), and the other from the layout of the picolinate moieties (absolute configuration Δ or Λ).[24] Indeed, the [Zn(bcpe)] complex crystallizes in the chiral *Pnn*2 orthorhombic space group, and only one enantiomer is found in the crystal [Λ(λ)]. However, it is surprising that despite its chirality, the [Cd(bcpe)] complex crystallizes in the $P2_1/n$ space group, which is not chiral. This is because the crystal contains a racemic mixture of both enantiomers [Λ(λ) and Δ(δ)], centrosymmetrically related.

X-Ray diffraction studies were also performed on a single crystal of the [Cd(bcpc)] complex. Fig. 2 shows a view of the structure of the complex, while bond lengths and angles of the Cd(II) coordination environment are listed in Table 1. The bond distances and angles of the metal coordination environment in [Cd(bcpc)] are very similar to those observed for the bpce analogue (Table 1). Thus, the replacement of the ethylene backbone of bcpe by a cyclohexylene ring does not substantially affect the coordination geometry around the Cd(II) ion. In [Cd(bcpc)] the cyclohexylene ring adopts a chair conformation (Fig. 2). The presence of a

cyclohexylene ring in bcpc prevents the λ→δ interconversion of the five-membered chelate ring formed upon coordination of the cyclohexylene diamino moiety, and therefore only one enantiomer is found in the crystal lattice [Λ(λ)].

The solid state structure of the Pb(II) complex of bcpe was also determined by single-crystal X-ray diffraction analyses. The crystals contain tetrameric structural units $[Pb_4(bcpe)_4]$ in which the four Pb(II) ions are bridged by carboxylate oxygen atoms. The asymmetric unit contains two of such units showing slightly different bond distances and angles of the metal coordination environment. Fig. 3 shows a view of a $[Pb_4(bcpe)_4]$ unit, while bond lengths and angles of the metal coordination environment are listed in Table 2. In the tetrameric unit each Pb(II) ion is directly bound to the six donor atoms of the ligand, seven coordination being completed by an oxygen atom of a neighbouring bcpe unit. The bond distances of the metal coordination environment of Pb(II), shown in Table 2, indicate an asymmetrical coordination of the metal ion by the ligand, with the Pb–N(3) bond distance [2.46(2) Å] being substantially shorter than the Pb–N(2) one [2.71(2) Å]. The distance between the metal ion and the oxygen atom of the neighbouring bcpe unit [Pb–O(3)#1 = 2.61(2) Å] is slightly longer than the Pb–O(2) distance [2.56(2) Å], but considerably shorter than the Pb–O(3) one [2.84(2) Å]. The tetrameric unit appears to be stabilized by face-to-face π–π stacking interactions between the pyridine rings of adjacent bcpe units (Fig. 3). These pyridine rings are nearly parallel to each other (1.6°), with a distance between the planes containing the aromatic rings of 3.29 Å, and a distance between centroids of 3.65 Å.

Table 2. Bond lengths (Å) and angles (°) of the metal coordination environment in $[Pb_4(bcpe)_4]$ (see Fig. 3 for numbering scheme).

Pb(1)–N(3)	2.46(2)	Pb(1)–N(1)	2.62(2)
Pb(1)–O(2)	2.56(1)	Pb(1)–N(2)	2.71(2)
Pb(1)–O(3)#1	2.61(1)	Pb(1)–O(3)	2.84(2)
Pb(1)–N(4)	2.61(2)		
N(3)–Pb(1)–O(2)	84.8(5)	O(2)–Pb(1)–N(2)	114.5(5)
N(3)–Pb(1)–O(3)#1	81.4(5)	O(3)#1–Pb(1)–N(2)	82.2(5)
O(2)–Pb(1)–O(3)#1	151.9(5)	N(4)–Pb(1)–N(2)	131.8(6)
N(3)–Pb(1)–N(4)	66.2(5)	N(1)–Pb(1)–N(2)	60.3(5)
O(2)–Pb(1)–N(4)	71.8(5)	N(3)–Pb(1)–O(3)	126.4(4)
O(3)#1–Pb(1)–N(4)	80.3(5)	O(2)–Pb(1)–O(3)	74.5(5)
N(3)–Pb(1)–N(1)	88.2(5)	O(3)#1–Pb(1)–O(3)	94.4(4)
O(2)–Pb(1)–N(1)	61.0(5)	N(4)–Pb(1)–O(3)	60.5(4)
O(3)#1–Pb(1)–N(1)	142.1(5)	N(1)–Pb(1)–O(3)	120.5(4)
N(4)–Pb(1)–N(1)	128.0(5)	N(2)–Pb(1)–O(3)	165.7(5)
N(3)–Pb(1)–N(2)	67.0(6)		

Symmetry transformations used to generate equivalent atoms: #1 $y - 1/2, -x + 1/2, -z + 1/2$.

It is well known that ligands containing two methylpicolinate moieties bridged by an ethylenediamine group may adopt two different conformations depending on the relative arrangement of the two pyridine units: twist–wrap (tw), in which the ligandwraps around the metal ion by twisting the pyridyl units relative to each other, and twist–fold (tf), where the twisting of the pyridyl units is accompanied by an overall folding of the two pyridine units.[25] Inspection of the X-ray crystal structures of the Zn(II), Cd(II) and Pb(II) complexes

shown in Fig. 2 and 3 indicate that while the Zn(II) and Cd(II) complexes present a tw conformation, the Pb(II) analogue shows a tf conformation in the solid state. As it can be seen in Fig. 3 the disposition of the donor atoms of the ligand around the Pb(II) ion results in an identifiable void. This is typical of the so-called hemi-directed compounds, in which the lone pair of electrons can cause a non-spherical charge distribution around the Pb(II) cation. Thus, the different structure observed for the Pb(II) complex of bcpe in the solid state when compared to that of the Zn(II) and Cd(II) analogues appears to be related to the stereochemical activity of the Pb(II) lone pair in the first compound.

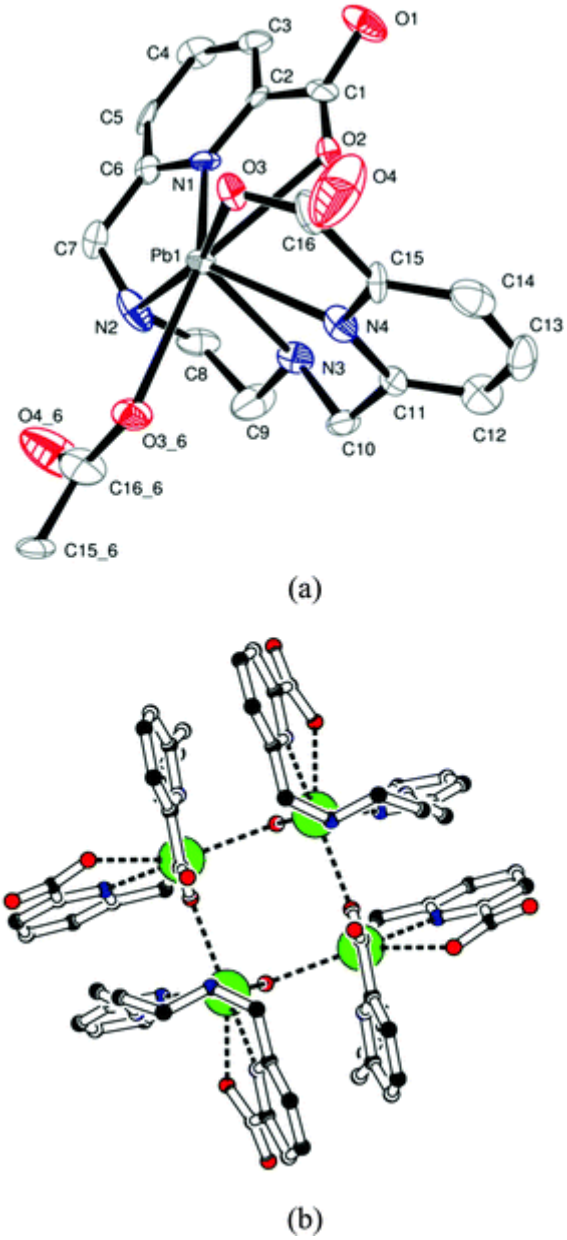

Fig. 3. (a) X-Ray crystal structure of $[Pb_4(bcpe)_4]$ with atom labelling; hydrogen atoms are omitted for simplicity. The ORTEP plots are drawn at the 30% probability level; (b) PLATON view of the $[Pb_4(bcpe)_4]$ unit.

Solution structure

The ^{1}H and ^{13}C NMR spectra of the Zn(II), Cd(II) and Pb(II) complexes of bcpe and bcpc were recorded from D_2O solution at 298 K (pD = 7.0), and assigned on the basis of two-dimensional COSY, NOESY, HSQC and HMBC experiments. The ^{1}H NMR spectra are shown in Fig. 4 and Figure S1 (ESI†), and the results are summarized in Table 3. The coordination of the bcpe andbcpc ligands to the metal ion causes important downfield shifts of the protons of the pyridine units. The spectra of the Zn(II) and Cd(II) complexes with a given ligand are very similar, indicating a similar structure of these complexes in solution. Thespectra of the complexes of bcpe consist of seven signals corresponding to the fourteen different proton magnetic environments of the ligand backbone (the proton signals due to the –NH groups are not observed), which points to an effective C_2 symmetry of the complexes in solution. This is confirmed by the ^{13}C NMR spectra, which show 8 signals for the 16 carbon nuclei of the ligand backbone (Table 3). A similar situation occurs for the Zn(II) and Cd(II) complexes of bcpc, the ^{1}H NMR spectra showing ten multiplets and the ^{13}C NMR spectra giving ten signals for the 20 carbon nuclei of the ligand backbone. Although the specific CH_2proton assignments of the H7ax/H7eq and H8ax/H8eq proton signals in the NMR spectra of [Zn(bcpe)] and [Cd(bcpe)] were not possible on the basis of the 2D NMR spectra, they were carried out using the stereochemically dependent proton shift effects, resulting from the polarization of the C–H bonds by the electric field effect caused by the cation charge.[26] This results in a deshielding effect of the H7eq and H8eq protons, which are pointing away from the M(II) ion (Table 3, see Scheme 1 for labelling). The methylene protons H7ax/H7eq yield AB spin patterns, while theprotons of the ethylenediamine units H8ax/H8eq give a AA′BB′ spectrum. The ^{1}H NMR spectra of the Zn(II) and Cd(II) complexes of bcpc also show an AB spin pattern for the H7ax/H7eq, where the signal due to the H7eq protons is again deshielded due to the polarization of the C–H bonds by the electric field effect caused by the cation charge.

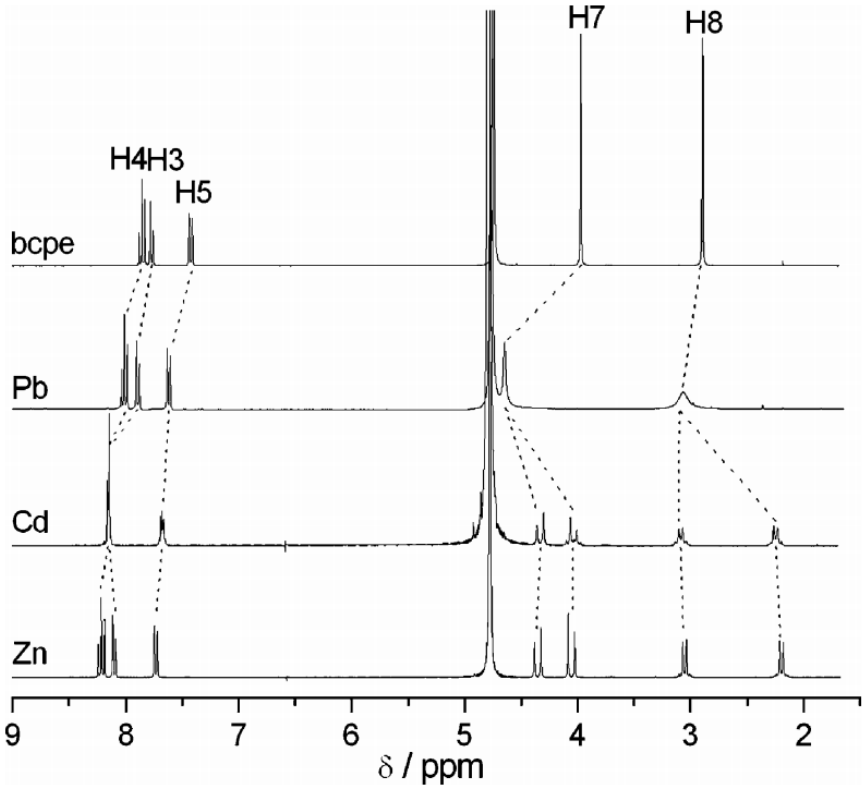

Fig. 4. ^{1}H NMR spectra of the bcpe ligand and [M(bcpe)] complexes (M = Zn, Cd or Pb) recorded from D_2O solutions at 298 K (pD = 7.0).

Table 3. ^{1}H and ^{13}C NMR shifts for the ligands H_2bcpe, H_2bcpc and their Zn, Cd and Pb complexes[a].

	H_4bcpe[a]	[Zn(bcpe)] [b]	[Cd(bcpe)] [c]	[Pb(bcpe)] [d]	H_4bcpc[e]	[Zn(bcpc)] [f]	[Cd(bcpc)] [g]	[Pb(bcpc)] [h]
H3	7.77	8.22	8.15	7.90	7.89	8.09	8.06	8.00
H4	7.86	8.11	8.15	8.02	7.96	8.21	8.12	8.11
H5	7.43	7.74	7.67	7.63	7.55	7.73	7.64	7.69
H7ax	3.97[i]	4.05	4.02	4.65 [i]	4.58(d)	4.25(m)	4.23(m)	4.54
H7eq		4.35	4.32	—	4.77(d)	—	—	5.04
H8ax	2.89[i]	2.20	2.24	3.06[i]	3.40	1.95	2.01	2.21
H8eq	—	3.05	3.07	—	—	—	—	—
H9ax	—	—	—	—	1.48	1.09(m)	0.97	0.95
H9eq	—	—	—	—	2.36	2.33	2.39	2.19
H10ax	—	—	—	—	1.19	1.09(m)	1.10	0.94
H10eq	—	—	—	—	1.77	1.68	1.68	1.59
C1	174.4	170.5	170.7	173.4	173.3	170.4	170.5	173.5
C2	154.7	148.1	149.2	152.0	152.8	148.1	149.1	152.2
C3	124.3	125.0	125.0	126.1	125.3	124.2	124.7	126.0
C4	140.2	144.0	143.2	141.9	141.0	143.9	143.0	142.1
C5	126.1	128.2	128.7	127.3	126.2	128.0	128.5	127.7
C6	156.8	158.8	156.0	158.9	154.0	155.8	158.3	157.5
C7	53.8	50.9	50.8	54.6	49.7	48.1	48.0	49.4
C8	47.4	49.3	49.8	51.7	60.2	61.7	61.5	62.1
C9	—	—	—	—	29.9	31.8	32.3	32.6
C10	—	—	—	—	24.4	25.9	26.0	26.0

[a] Conditions: T = 298 K. D_2O. 300 MHz. pD = 7.0. Assignment supported by 2D H–H COSY, HSQC and HMBC experiments. $^{3}J_{3-4}$ = 7.7 Hz; $^{4}J_{3-5}$ = 0.90 Hz; $^{3}J_{5-4}$ = 7.6 Hz. [b] $^{2}J_{7ax-7eq}$ = 17.2 Hz; $^{2}J_{8ax-8eq}$ = 10.0 Hz; $^{3}J_{3-4}$ = 7.6 Hz; $^{3}J_{5-4}$ = 7.8 Hz; $^{4}J_{3-5}$ = 7.6 Hz. [c] $^{2}J_{7ax-7eq}$ = 17.0 Hz; $^{2}J_{8ax-8eq}$ = 10.0 Hz; $^{3}J_{5-4}$ = 5.6 Hz; $^{4}J_{5-3}$ = 3.2 Hz. [d] $^{3}J_{3-4}$ = 7.2 Hz; $^{3}J_{5-4}$ = 7.6 Hz. [e] $^{3}J_{3-4}$ = 7.2 Hz; $^{3}J_{5-4}$ = 7.5 Hz, $^{2}J_{7ax-7eq}$ = 16.5 Hz; $^{2}J_{9ax-9eq}$ = 12.9 Hz; $^{2}J_{10ax-10eq}$ = 8.8 Hz. [f] $^{2}J_{7ax-7eq}$ = 17.3 Hz; $^{2}J_{9ax-9eq}$ = 11.8 Hz; $^{2}J_{10ax-10eq}$ = 7.6 Hz; $^{3}J_{3-4}$ = 7.5 Hz; $^{3}J_{5-4}$ = 7.8 Hz. [g] $^{2}J_{9ax-9eq}$ = 12.4 Hz; $^{2}J_{10ax-10eq}$ = 8.0 Hz; $^{3}J_{3-4}$ = 7.1 Hz; $^{3}J_{5-4}$ = 7.3 Hz. [h] $^{2}J_{7ax-7eq}$ = 16.6 Hz; $^{3}J_{3-4}$= 7.6 Hz; $^{3}J_{5-4}$ = 7.7 Hz. [i] Axial and equatorial protons give a single ^{1}H NMR signal.

The ^{1}H NMR spectrum of [Pb(bcpe)] is quite different to those of the Zn and Cd analogues (Fig. 4). At room temperature the signals due to the H7 and H8 protons in [Pb(bcpe)] are observed as broad signals, in contrast to the AB and AA′BB′ spectraobserved in the case of the Zn and Cd complexes. Thus, the ^{1}H NMR spectrum of [Pb(bcpe)] is in agreement with an effective C_{2v} symmetry of the complex in solution. This indicates that the Pb complex presents a more flexible structure in solution than the Zn and Cd analogues, which could be related to the presence of a stereochemically active 6s lone pair in the case of the Pb complex. The signal due to the H7 protons indicate an important downfield shift upon coordination to Pb(II) (0.68 ppm). The remaining proton signals, which undergo downfield shifts of 0.13–0.20 ppm, are less affected by the coordination of the ligand to the metal ion. The ^{1}H NMR spectrum of the [Pb(bcpc)] complex also shows important differences with respect to the spectra of the Zn and Cd analogues, in particular with regard to the position of the H7 and H8 signals. This again suggests that the Pb complex possesses a different structure in solution.

DFT studies

In light of the X-ray diffraction analysis, the Pb(II) complex of bcpe presents a tetrameric structure in the solid state where oxygen atoms of the carboxylate groups act as bridging ligands between four Pb(II) ions (see above). However, it is unlikely that this tetrameric structure is maintained in aqueous solution. Thus,

aiming to obtain information about the structure of the Pb(II) complexes of bcpe and bcpc in solution, as well as to investigate the possible stereochemical activity of the Pb(II) lone pair, the [Pb(L)] systems (L = bcpe or bcpc) were characterized by means of DFT calculations (B3LYP model). On the grounds of our previous experience[27,28] in these calculations, the 6–31G(d) basis set was used for the ligand atoms, while for the metals the effective core potential of Wadt and Hay (Los Alamos ECP) included in the LanL2DZ basis set was applied. This ECP has been demonstrated to provide reliable results for different Pb(II) coordination compounds.[29–31] Compared to the all-electron basis sets, ECPs account for relativistic effects to some extent. It is believed that relativistic effects will become important for the elements from the fourth row of the periodic table.

Geometry optimizations of the [Pb(L)] systems (L = bcpe or bcpc) provide two different minimum energy geometries where the ligand adopts different conformations (Fig. 5): twist–wrap (tw), in which the ligand wraps around the metal ion by twisting the pyridyl units relative to each other, and twist–fold (tf), where the twisting of the pyridyl units is accompanied by an overall folding of the two pyridine units. The optimized bond distances and angles of the metal coordination environments of both conformations are given in Table 4. Both minimum energy structures are true energy minima because the vibrational frequency analyses give no imaginary frequencies. The tf conformations show smaller N(1)–Pb–N(4) angles than the tw ones, while the O(2)–Pb–O(3) angles are close to 180° in the tw conformations, and *ca.* 85° in the tf ones. The results shown in Table 4 indicate that the substitution of the ethane-1,2-diamine of bcpe by a cyclohexane-1,2-diamine group does not substantially affect the bond distances and angles of the metal coordination environment.

Table 4. The calculated (B3LYP/6–31G*) bond lengths (Å) and angles (°) of the Pb(II) coordination environment obtained for the [Pb(bcpe)] and [Pb(bcpc)] systems. (See Fig. 3 for numbering scheme.)

	[Pb(bcpe)]		[Pb(bcpc)]	
	tw	tf	tw	tf
Pb–N(1)	2.534	2.803	2.523	2.716
Pb–N(2)	2.549	3.322	2.540	3.206
Pb–N(3)	2.549	2.764	2.540	2.819
Pb–N(4)	2.534	2.469	2.522	2.456
Pb–O(2)	2.519	2.206	2.529	2.222
Pb–O(3)	2.519	2.248	2.529	2.257
N(1)–Pb–N(4)	142.13	130.06	142.46	130.92
O(2)–Pb–O(3)	178.53	85.95	178.99	84.96

The optimized geometries for the tw conformations show nearly undistorted C_2 symmetries (Table 4), while in the tf forms the metal ion is asymmetrically coordinated by the ligand. Moreover, the calculated Pb–N(2) distances of tf conformations are considerably longer than the remaining bond distances of the metal coordination environment. This suggests an important degree of stereochemical activity of the Pb(II) lone pair in tf conformations. An analysis of the natural bond orbitals (NBOs) in the tw and tf conformations of the [Pb(bcpe)] and [Pb(bcpc)] complexes (Table 5) shows that the Pb(II) lone pair orbital possesses a predominant 6s character, but it is polarized by a substantial 6p contribution in both tw (*ca.* 3.8%) and tf (*ca.* 5.2%) conformations. Similar p contributions (1.89–4.39%) have been calculated for different hemi-directed four-coordinate Pb(II) complexes with neutral ligands, while p contributions in the range 2.62–15.72% have been calculated for hemi-directed four-coordinate Pb(II) complexes with anionic ligands.[16] Moreover, the distribution of the ligand donor atoms around the Pb(II) ion is far from being spherical, a void

in the ligand geometry being clearly observed in both tw and tf conformations (Fig. 5). These results clearly confirm that the Pb(II) lone pair is stereochemically active in these complexes, the stereochemical activity being more important for the tf conformations than for the tw ones.

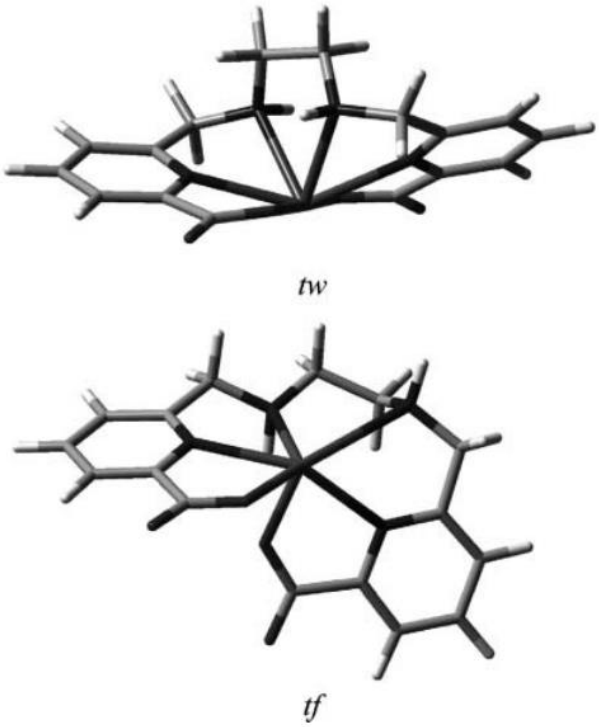

Fig. 5. Molecular geometries of the twist–wrap (tw) and twist–fold (tf) isomers of [Pb(bcpe)] obtained from DFT calculations.

The relative energies of the tw conformation with respect to the tf ones in [Pb(bcpe)] and [Pb(bcpc)] complexes were calculated both *in vacuo* ($\Delta G°$) and in aqueous solution (ΔG^{sol}). In the latter calculations, solvent effects were included by using a polarizable continuum model (C-PCM). The relative free energies were calculated as $\Delta G = G_{(tf)} - G_{(tw)}$, and therefore a positive relative energy indicates that the tw conformation is more stable than the tf conformation. Our calculations provide *in vacuo* relative energies of $\Delta G° = -5.12$ and -3.09 kcal mol^{-1} for [Pb(bcpe)] and [Pb(bcpc)] complexes, respectively, while in aqueous solution $\Delta G^{sol} = -15.21$ for [Pb(bcpe)] and -3.00 kcal mol^{-1} for [Pb(bcpc)]. Thus, our calculations predict that the tf conformation is more stable than the tw conformation both *in vacuo* and in aqueous solution for both the bcpe and the bcpc complexes. These results are in agreement with the solid state structure of the [Pb(bcpe)] complex described above, for which a tf conformation is observed. However, the increased rigidity of bcpc when compared to bcpe provokes an important stabilization of the tw conformation.

Table 5. Natural bond orbital (NBO) analyses of the Pb(II) lone pair for [Pb(bcpe)] and [Pb(bcpc)] complexes.

	tw	tf
[Pb(bcpe)]	s[96.24%]p0.04[3.76%]	s[94.76%]p0.06[5.26%]
[Pb(bcpc)]	s[96.12%]p0.04[3.88%]	s[94.82%]p0.05[5.18%]

Ligand protonation constants and stability constants of the metal complexes

The protonation constants of the ligands bcpe and bcpc as well as the stability constants of its metal complexes formed with different metal ions (Zn(II), Cd(II), Pb(II) and Ca(II)) were determined by potentiometric titrations. The titration curves of the twoligands and their metal complexes are shown in Fig. 6. The constants and standard deviations are given in Table 6, which also lists the protonation and stability constants reported for the related systems: edta, cdta, bped and dpaea (Scheme 3). The ligand protonation constants are defined as in eqn 1, and the stability constants of the metal chelates are expressed in eqn 2, with L = bcpe or bcpc.

$$K_i = \frac{[\mathrm{H}_i\mathrm{L}]}{[\mathrm{H}_{i-1}\mathrm{L}][\mathrm{H}^+]} \quad (1)$$

$$K_{\mathrm{ML}} = \frac{[\mathrm{ML}]}{[\mathrm{M}][\mathrm{L}]} \quad (2)$$

The titrations of H_2bcpe and H_2bcpc (Fig. 6) are indicative of two fairly strongly acidic sites and two weakly acidic sites. In comparison with edta, the bcpe and bcpc ligands have lower protonation constants for the first protonation step, while the second protonation constants are similar to that observed for edta. These two protonation steps occur on the amine nitrogen atoms. As previously observed,[32] C-alkylation of the ethylenediamine unit causes a slight increase of the basicity of the aminenitrogen atoms due to inductive effects of the added alkyl groups. The last two protonation steps probably take place at the pyridylcarboxylate groups, the protonation constants determined for bcpe and bcpc being very similar to the second and third protonation constants reported for dpaea.[17]

Table 6. Ligand protonation constants and thermodynamic stability constants of bcpe and bcpc and its metal complexes as determined by pH potentiometry [I = 0.1 M (Me_4N)(NO_3)]. Data reported previously for related systems are provided for comparison.

	Bcpe	Bcpc	Edta[a]	Cdta [b]	Bped [c]	Dpaea [d]
logK_1	8.69(1)	9.13(2)	10.19	12.3	8.84	8.15
logK_2	6.18(2)	6.44(5)	6.13	6.11	5.63	3.5
logK_3	3.08(2)	3.25(7)	2.69	3.49	3.02	2.6
logK_4	2.33(3)	2.40(7)	2.00	2.4	2.34	—
logK_{ZnL}	15.62(1)	15.87(4)	16.5	19.3	15.2	[e]
logK_{CdL}	14.45(1)	15.89(1)	16.5	19.7	14.6	[e]
logK_{PbL}	12.68(1)	15.00(2)	18.0	20.2	[e]	12.1
logK_{CaL}	5.81(1)	6.07(7)	10.6	13.1	[e]	5.5
Cd/Ca selectivity	$10^{8.6}$	$10^{9.8}$	$10^{5.9}$	$10^{6.6}$	—	[e]
Pb/Ca selectivity	$10^{6.9}$	$10^{8.9}$	$10^{7.4}$	$10^{7.1}$	—	$10^{6.6}$

[a] Ref. 33 and Ref. 34. [b] Ref. 33 and Ref. 34. [c] Ref. 34. [d] Ref. 17. [e] Not determined.

The 1 : 1 titration curves with all metal ions (Fig. 6) display an inflection at $a = 4$ (a = mol of OH^-/mol of ligand), as expected for the formation of [M(bcpe)] and [M(bcpc)] species (M = Pb, Cd, Zn or Ca). The potentiometric data do not indicate the presence of significant amounts of the soluble hydroxide complexes in the pH range investigated. The two ligands form stable Zn(II), Cd(II) and Pb(II) chelates in aqueous solution. The stability constants determined for the Zn(II) and Cd(II) complexes are 1–2 log$K$ units lower than those of the corresponding edta complexes,[33] and are very similar to those reported for bped.[34]However, the stability constant determined for [Pb(bcpe)] is *ca.* 5.3 log$K$ units lower than that determined for the edta analogue. The stability constants determined for bcpe follow the trend: Zn(II) > Cd(II) > Pb(II) >> Ca(II). This behaviour contrasts with that observed for edta, for which the stability constants of the metal complexes vary in the following order: Pb(II) > Cd(II) ~ Zn(II) >> Ca(II).[33]

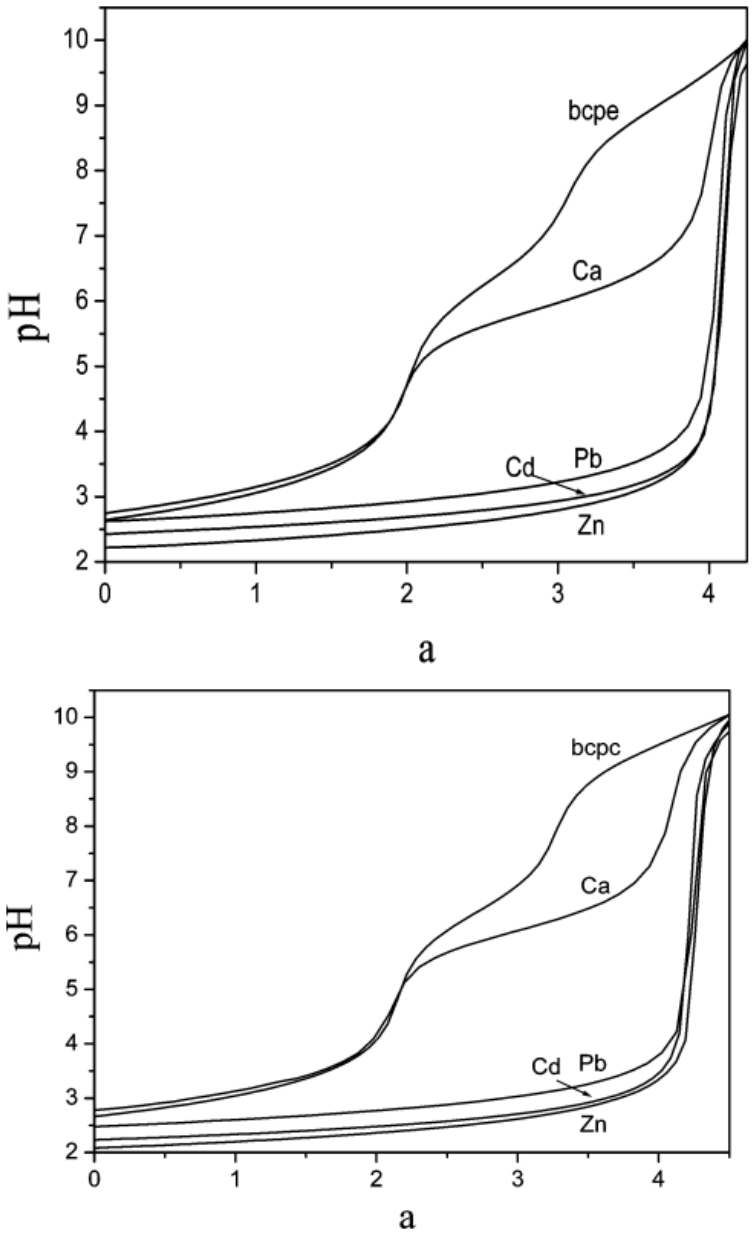

Fig. 6. Titration curves (pH *vs.a*; a = mol of OH^-/mol ligand) for H_2bcpe·2HCl (top) and H_2bcpc·3HCl (bottom) in the presence and absence of equimolar Pb(II), Cd(II), Zn(II) or Ca(II); $[L]_{tot} = 2 \times 10^{-3}$ M.

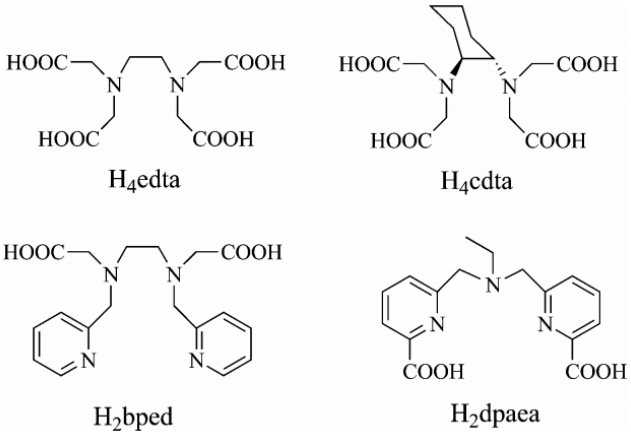

Scheme 3

It is well known that the replacement of the ethylene backbone with a cyclohexylene ring increases complex stability of some divalent and trivalent transition metal complexes,[32] while in the case of lanthanide(III) ions the introduction of a cyclohexyl ring in the ligand backbone decreases the stability of the complexes.[25,35] A comparison of the complex stabilities of the edta and cdta complexes (Table 6) shows that the introduction of a cyclohexylene ring increases the stability of the corresponding Zn(II), Cd(II), Pb(II) and Ca(II) complexes by 0.2–2.3 log*K* units. The results shown in Table 6 indicate that the replacement of the ethylene backbone of bcpe by a cyclohexylene ring causes a very important increase of the stability constant of the Pb(II) complex (*ca*. 2.3 log*K* units), while this effect is less important for Cd(II) (*ca.* 1.4 log*K* units). However, the introduction of the cyclohexylene ring does not substantially affect the stability of the Zn(II) and Ca(II) complexes. As a consequence, the stabilities of the Pb(II), Cd(II) and Zn(II) complexes of bcpc are very similar. Thus, the replacement of the ethylene backbone with a cyclohexylene ring in bcpe shifts the selectivity towards the larger Pb(II) ion, whereas the opposite trend is observed for edta. This may be attributed to the different topology of the bcpe and edta ligands. Part of the increase in stability of the Pb(II) complex upon introduction of the cyclohexylene ring is due to the greater basicity of bcpc($\Sigma\log\{[H_i\text{bcpc}]/[H_{i-1}\text{bcpc}][H^+]\}$ = 21.2) over that of bcpe ($\Sigma\log\{[H_i\text{bcpce}]/[H_{i-1}\text{bcpe}][H^+]$ = 20.3). However, most of the increase is probably an entropic effect due to the greater pre-organization of the donor groups of bcpc over those of bcpe. Indeed, ^{1}H NMR studies indicate that the [Pb(bcpc)] complex possesses a more rigid coordination environment than the corresponding bcpe complex (see above).

The replacement of the ethylene backbone in bcpe with a cyclohexylene ring has an strong effect on the selectivity for Pb(II) and Cd(II) over Ca(II), with bcpc showing Pb/Ca and Cd/Ca selectivities of $10^{8.9}$ and $10^{9.8}$, respectively, superior to the extracting agents already used in Pb(II) and Cd(II) removal from contaminated water and soils such as edta (Table 6).[36] The speciation diagrams shown in Fig. 7 highlight the selectivities of both the ligands for Pb and Cd over Ca. For instance, Pb(II) and Cd(II) complexes of bcpc are almost totally formed at pH 4.0 (99.4 and 99.8%, respectively), while only 0.003% of the total Ca(II) is complexed under the same conditions.

Conclusions

The hexadentate ligands bcpe and bcpc form thermodynamically stable Zn(II), Cd(II) and Pb(II) complexes in aqueous solution, and thus can be considered as new basic structural frameworks for the design of novel Cd(II) and Pb(II) extracting agents. Our results show an improved Pb/Ca and Cd/Ca selectivity in aqueous solution when the ethyl group of bcpe is replaced by a cyclohexyl unit. The ligand bcpc shows Pb/Ca and

Cd/Ca selectivities of $10^{8.9}$ and $10^{9.8}$, respectively, superior to the extracting agents already used in Pb(II) and Cd(II) removal from contaminated water and soils, such as edta.[36]Single-crystal X-ray diffraction studies in the solid state and ^{1}H and ^{13}C NMR studies in D_2O solution indicate hexadentate binding of bcpe and bcpc to Zn(II), Cd(II) and Pb(II). Structural analysis and quantum mechanical calculations performed at the DFT level indicate that the Pb(II) complexes present a somewhat different structure in comparison with the Zn(II) and Cd(II) analogues, which it is attributed to the stereochemical activity of the Pb(II) lone pair. Indeed, the analysis of the natural bond orbitals (NBOs) indicate that the Pb(II) lone pair is polarized by a substantial 6p contribution, which results in a hemi-directed coordination geometry around the metal ion.

Experimental

General considerations

1,2-Bis{[[6-(methoxycarbonyl)pyridin-2-yl]methyl]amino}-ethane (**2a**)[19] and (1*R*,2*R*)-{[[6-(methoxycarbonyl)pyridin-2-yl]methyl]amino}-cyclohexane (**2b**)[37] were prepared as previously reported by us. All other chemicals were purchased from commercial sources and used without further purification. Solvents were of reagent grade purified by the usual methods.

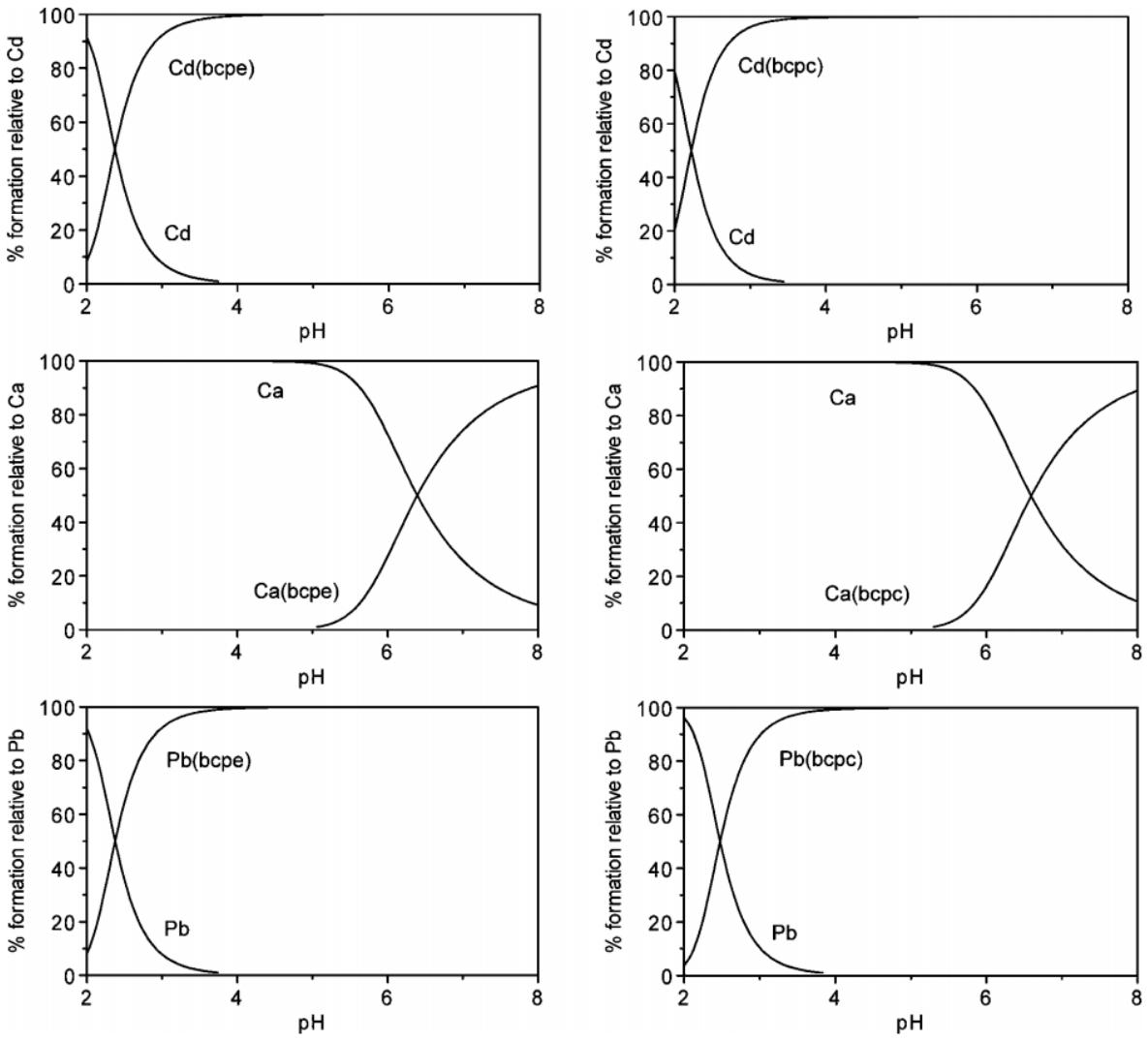

Fig. 7. Lead, cadmium and calcium speciation in the presence of bcpe and bcpc. $[M^{2+}]_{tot} = [L]_{tot} = 10^{-3}$ M.

Caution! Although we have experienced no difficulties with the perchlorate salts, these should be regarded as potentially explosive and handled with care.[38]

Elemental analyses were carried out on a Carlo Erba 1180 elemental analyzer and FAB-MS were recorded on a FISONS QUATRO mass spectrometer with a Cs ion gun using 3-nitrobenzyl alcohol as the matrix. IR spectra were recorded, as KBr discs, using a Bruker Vector 22 spectrophotometer. ^{1}H and ^{13}C NMR spectra were obtained using a Bruker Avance 300 or Bruker Avance 500 spectrometer. Chemical shifts are reported in δ values. For measurements in D_2O, *tert*-butyl alcohol was used as an internal standard with the methyl signal calibrated at $\delta = 1.2$ (^{1}H) and 31.2 ppm (^{13}C). Spectral assignments were based, in part, on two-dimensional COSY, HMQC and HMBC experiments. Samples of the Zn(II), Cd(II) and Pb(II) complexes of bcpe and bcpc for NMR measurements were prepared by dissolving equimolar amounts of the ligand and hydrated $M(ClO_4)_2$ (M = Zn or Cd) or $Pb(NO_3)_2$ in D_2O, followed by an adjustment of the pD with ND_4OD and DCl (Aldrich) solutions in D_2O.

Potentiometry

Ligand protonation constants and stability constants with Zn(II), Cd(II), Pb(II) and Ca(II) were determined by pH potentiometric titration at 25 °C in 0.1 M tetramethylammonium nitrate. The titrations were carried out by adding a standardized tetramethylammonium hydroxide solution with a Metrohm Dosimat 794 automatic burette. A glass electrode filled with 3 M KCl was used to measure the pH. The stock solutions were prepared by dilution of the appropriate standards. The exact amount of acid present in the standard solutions was determined by pH measurement. Tetramethylammonium hydroxide was standardized by potentiometric titration against potassium hydrogen phthalate. H_2bcpe and H_2bcpc were checked for purity by NMR and elemental analysis before titration. The ligand and metal–ligand (1 : 1) solutions were titrated over the pH range 2.2 < pH < 11.0. The protonation and stability constants were calculated from simultaneous fits of three independent titrations with the program HYPERQUAD.[39] The errors given correspond to one standard deviation.

Synthesis

1,2-Bis{[[6-(carboxy)pyridin-2-yl]methyl]amino}-ethane dichlorohydrate (H_2bpce·2HCl). 1,2-Bis{[[6-(methoxycarbonyl)pyridin-2-yl]methyl]amino}-ethane (0.478 g, 1.35 mmol) was dissolved in 6 M hydrochloric acid, and the mixture heated to reflux for 24 h. The white precipitate formed was isolated by filtration, washed with acetone and air dried (yield: 0.290 g, 53%). Anal. calcd. for $C_{16}H_{20}N_4O_4$·2HCl: C 47.65, H 5.00, N 13.89. Found: C 47.46, H 5.08, N 13.81. FAB-MS (*m*/*z* (%BPI)): 331(100) $[H_3bpce]^+$. IR(KBr): 1761 ν(C=O), 1620 ν(C=N), 1584 ν(C=C) cm^{-1}. X-Ray quality crystals of H_2bpce·2HCl were grown by slow evaporation of the mother liquor.

1,2-Bis{[[6-(carboxy)pyridin-2-yl]methyl]amino}-ethane dinitratehydrate (H_2bcpe·2HNO_3·H_2O). A 0.1035 M solution of $Ag(NO_3)$ inwater (10 cm^3) was added to a solution of 0.208 g of H_2bpce·2HCl in the same solvent (15 cm^3). The white precipitate of AgCl was filtered off and the filtrate was concentrated to dryness to give the desired product as a white solid (yield: 0.202 g, 82%). Anal. calcd. for $C_{16}H_{20}N_4O_4$·2HNO_3·H_2O: C 40.51, H 4.67, N 17.72. Found: C 40.32, H 4.22, N 17.75. FAB-MS (*m*/*z* (%BPI)): 331(100) $[H_3bpce]^+$. IR (KBr): 1762 ν(C=O), 1598, $\nu(C{=}N)_{py}$, 1552 $\nu(C{=}C)_{py}$ cm^{-1}.

(1*R*,2*R*)-{[[6-(carboxy)pyridin-2-yl]methyl]amino}-cyclohexane (H_2bcpc·3HCl). $NaBH_4$ (0.0072 g, 0.191 mmol) was added to a stirred suspension of (1*R*,2*R*)-{[[6-(methoxycarbonyl)pyridin-2-yl]methylene]amino}-cyclohexane (0.390 g, 0.955 mmol) inmethanol (40 cm^3) at 0 °C. The mixture was stirred at 0 °C for 20 min and then a saturated $NaHCO_3$ solution (100 cm^3) was added. The resulting solution was extracted with CH_2Cl_2 (5 × 150 cm^3). The combined organic extracts were dried over $Na_2SO_4$and evaporated. The residue was dissolved in 6 M HCl, and the mixture heated to reflux for 24 h. The white precipitate formed was isolated by filtration, washed with acetone and air dried (yield: 0.174 g, 47%). Anal. calcd. for $C_{16}H_{20}N_4O_4$·3

HCl: C 48.64, H 5.51, N 11.35. Found: C 48.06, H 5.83, N 10.92. FAB-MS (*m*/*z* (%BPI)): 385(65) $[H_3bcpc]^+$. IR (KBr): 1770 ν(C=O), 1605 $\nu(C{=}N)_{py}$, 1575 $\nu(C{=}C)_{py}$ cm^{-1}.

[Zn(bcpe)]·3H$_2$O (1). A 0.101 g amount of $H_2bcpe{\cdot}2HCl$ (0.250 mmol) was suspended in 20 cm^3 of a 2-propanol–MeOH mixture (3 : 1) and triethylamine (140 μL, 1.004 mmol) was added. The mixture was heated to reflux and 2 cm^3 of an aqueous solution of $Zn(ClO_4)_2{\cdot}6H_2O$ (0.111 g, 0.306 mmol) was added. The resulting solution was refluxed for 1 h. Slow evaporation of this solution gave colourless crystals suitable for X-ray diffraction analyses (0.059 g, 42%). Anal. calcd. for $C_{16}H_{18}N_4O_4Zn{\cdot}3H_2O$: C 42.92, H 4.95, N 12.51. Found: C 42.47, H 4.91, N 12.36. FAB-MS (*m*/*z* (%BPI)): 393(100) $[Zn(L + H)]^+$. IR (KBr): 1627 $\nu_a(C{=}O)$, 1593 $\nu(C{=}C)_{py}$, 1382 $\nu_s(C{=}O)$ cm^{-1}.

[Cd(bcpe)]·2H$_2$O (2). A 0.088 g amount of $H_2bcpe{\cdot}2HCl$ (0.218 mmol) was suspended in 20 cm^3 of a 2-propanol–MeOH mixture (3 : 1) and triethylamine (122 μL, 0.875 mmol) was added. The mixture was heated to reflux and 2 cm^3 of an aqueous solution of $Cd(ClO_4)_2{\cdot}4H_2O$ (0.085 g, 0.273 mmol) was added. The resulting solution was refluxed for 1 h and then left to cool to room temperature. The white precipitate formed was isolated by filtration and air dried (0.054 g, 52%). Anal. calcd. for $C_{16}H_{18}CdN_4O_4{\cdot}2H_2O$: C 40.31, H 4.23, N 11.75. Found: C 39.68, H 4.12, N 11.51. FAB-MS (*m*/*z* (%BPI)): 443(100) $[Cd(L + H)]^+$. IR(KBr): 1627 $\nu_a(C{=}O)$, 1589 $\nu(C{=}C)_{py}$, 1377 $\nu_s(C{=}O)$ cm^{-1}. Colourless X-ray quality crystals were grown by slow evaporation of the mother liquor.

[Pb(bcpe)]·2H$_2$O (3). A 0.104 g amount of $H_2bcpe{\cdot}2HNO_3{\cdot}H_2O$ (0.219 mmol) was suspended in 20 cm^3 of a 2-propanol–MeOH mixture (3 : 1) and triethylamine (123 μL, 0.883 mmol) was added. The mixture was heated to reflux and $Pb(NO_3)_2$(0.073 g, 0.220 mmol), dissolved in water (3 cm^3), was added. The resulting solution was refluxed for 1 h and then left to cool to room temperature. The white precipitate formed was isolated by filtration and air dried (0.046 g, 39%). Anal. calcd. for $C_{16}H_{18}N_4O_4Pb{\cdot}2H_2O$: C 33.62, H 3.53, N 9.80. Found: C 32.27, H 3.44, N 9.99. FAB-MS (*m*/*z* (%BPI)): 537(100) $[Pb(L + H)]^+$. IR(KBr): 1618 $\nu_a(C{=}O)$, 1583 $\nu(C{=}C)_{py}$, 1384 $\nu_s(C{=}O)$ cm^{-1}. Colourless X-ray quality crystals were grown by slow diffusion ofacetone into a solution of the isolated solid in methanol.

Crystal structure determinations

Three-dimensional X-ray data for $H_2bcpe{\cdot}2HCl$, [Zn(bcpe)] and [Cd(bcpe)] were collected on a Bruker SMART 1000 CCD diffractometer by omega and phi rotation with narrow frames. Reflections were measured from a hemisphere of data collected of frames each covering 0.3 degrees in omega. Of the 11 928, 13 474 and 19 812 reflections measured for $H_2bcpe{\cdot}2HCl$, [Zn(bcpe)] and [Cd(bcpe)], respectively, all of which were corrected for Lorentz and polarisation effects and for absorption by semi-empirical methods based on symmetry-equivalent and repeated reflections, 1636, 3285 and 3810 independent reflections exceeded the significance level $|F|/\sigma(|F|) > 2.0$. The solution, refinement and analysis of the single-crystal X-ray diffraction data was performed with the WinGX suite for small molecule single-crystal crystallography.[40] The structure of $H_2bcpe{\cdot}2HCl$ was solved by direct methods with SHELXS-97,[41] the structure of [Zn(bcpe)] was solved with DIRDIF-99[42] by Patterson methods and that of [Cd(bcpe)] was solved with SIR92[43] by direct methods. All structures were refined by full-matrix least-squares methods on F^2 with SHELX-97.[41] The hydrogen atoms were included in calculated positions and refined by using a riding mode, except those bound to the water molecules in [Zn(bcpe)] and [Cd(bcpe)] that were found in the electron density map and the distance to the oxygen atom fixed. The refinement converged with the allowance for thermal anisotropy of all non-hydrogen atoms.

Three-dimensional X-ray data for $[Pb_4(bcpe)_4]$ were collected on a Bruker X8 Kappa APEXII CCD diffractometer. The data were corrected for Lorentz and polarization effects and for absorption by semiempirical methods[44] based on symmetry-equivalent and repeated reflections. Complex scattering factors were taken from the program SHELX-97[41] included in the WinGX program system[40] as implemented on a

Pentium® computer. The structure was solved by Patterson methods (DIRDIF-99)[42] and refined[41] by full-matrix least-squares on F^2. All hydrogen atoms were included in calculated positions and refined in riding mode. The crystal was of low quality. It was a twined crystal with many secondary domains together with the main one, and any attempt to find the twin law failed. Thus, to get better results we decided to use the program SQUEEZE implemented in the PLATON[45] program system to clean up some of the residual Q peaks probably associated with the secondary domains of the twin. The refinement converged with anisotropic displacement parameters for all non-hydrogen atoms after imposing 171 restraints.

Colourless X-ray quality crystals of [Cd(bcpc)] (**4**) were obtained by reacting H_2bcpc with a stoichiometric amount of $Cd(ClO_4)_2 \cdot 4H_2O$ in methanol. The mixture was heated to reflux for 1 h, the solvent was removed in a rotary evaporator, and the resulting solid was re-dissolved in 2-propanol. The slow diffusion of diethylether into this solution afforded single crystals suitable for X-ray diffraction analyses. Three-dimensional X-ray data for this crystal were collected on a Bruker X8 Kappa APPEXII CCD diffractometer. The data were corrected for Lorentz and polarization effects and for absorption by semiempirical methods[44] based on symmetry-equivalent and repeated reflections. The structure was solved with SIR92[43] by direct methods and refined by full-matrix least-squares methods on F^2 with SHELX-97.[41] All hydrogen atoms were included in calculated positions and refined in riding mode. The refinement converged with the allowance for thermal anisotropy of all non-hydrogen atoms. The crystal data and details on data collection and refinement are summarized in Table 7.

Table 7. Crystal data and structure refinements[a]

	H_2bcpe·2HCl	1	2	3	4
Formula	$C_{16}H_{20}Cl_2N_4O_4$	$C_{16}H_{22}N_4O_7Zn$	$C_{16}H_{20}N_4O_6Cd$	$C_{64}H_{64}N_{16}O_{16}Pb_4$	$C_{20}H_{22}CdN_4O_4$
MW	403.26	447.75	476.76	2142.11	494.82
Space group	$P2_1/c$	$Pnn2$	$P2_1/n$	$I\bar{4}$	$P2_12_12_1$
Crystal system	Monoclinic	Orthorhombic	Monoclinic	Tetragonal	Orthorhombic
a/Å	14.263(2)	11.4629(5)	10.919(2)	26.931(2)	10.3652(4)
b/Å	7.8583(9)	15.4564(7)	10.220(2)	26.931(2)	10.4820(5)
c/Å	8.125(1)	10.6802(5)	16.454(3)	11.473(2)	17.8467(8)
β/°	92.341(2)	90	93.284(3)	90	90
V/Å^3	909.9(2)	1892.3(1)	1833.1(6)	8321(1)	1939.0(2)
Z	2	4	4	4	4
T/K	298.0(1)	100.0(2)	100.0(2)	100.0(2)	100.0(2)
λ (Mo Kα)/Å	0.71073	0.71073	0.71073	0.71073	0.71073
D_{calcd} /g cm^{-3}	1.472	1.572	1.728	1.71	1.695
μ/mm^{-1}	0.387	1.345	1.233	8.134	1.162
R_{int}	0.0358	0.035	0.0384	0.1295	0.0350
Reflections measured	2270	3693	4532	4323	3946
Reflections observed	1636	3285	3810	3267	3704
R_1 [a]	0.0345	0.0276	0.0475	0.0522	0.0219
R_1 (all data)[a]	0.059	0.0341	0.058	0.0694	0.0248
wR_2 [b]	0.0722	0.0602	0.1168	0.1187	0.0455
wR_2 (all data)[b]	0.0901	0.0621	0.1206	0.1255	0.0469

[a] $R_1 = \sum||F_o| - |F_c||/\sum|F_o|$. [b] $wR_2 = \{\sum[w(|F_o|^2 - |F_c|^2)^2]/\sum[w(F_o^4)]\}^{1/2}$.

Computational details

The [Pb(L)] systems (L = bcpe or bcpc) were fully optimized by using the B3LYP density functional model.[46,47] In these calculations we have used the standard 6–31G(d) basis set for the ligand atoms, while the LanL2DZ valence and effective core potential functions were used for Pb.[48,49] The stationary points found on the potential energy surfaces as a result of the geometry optimizations of the complexes have been tested to represent energy minima rather than saddle points *via* frequency analysis. The relative free energies of the twist–wrap (tw) and twist–fold (tf) conformations of [Pb(L)] (L = bcpe or bcpc) complexes were calculated *in vacuo* including non-potential energy (NPE) contributions (that is, zero-point energy and thermal terms) obtained by frequency analysis. In aqueous solution, the relative free energies of the tw and tf conformations were calculated from solvated single-point energy calculations on the geometries optimized *in vacuo*. Solvent effects were evaluated by using the polarizable continuum model (PCM). In particular, we used the C-PCM variant[50] that employs conductor rather than dielectric boundary conditions. The solute cavity is built as an envelope of spheres centred on atoms or atomic groups with appropriate radii. The calculations were performed using an average area of 0.2 $Å^2$ for all the finite elements (tesserae) used to build the solute cavities. Final free energies include both electrostatic and non-electrostatic contributions. The wave functions of the complexes were analyzed by natural bond orbital analyses, involving natural atomic orbital (NAO) populations and natural bond orbitals (NBO).[51,52] All DFT calculations were performed by using the Gaussian 03 (Revision C.01) program package.[53]

Acknowledgements

The authors thank Xunta de Galicia (PGIDIT06TAM10301PR) for generous financial support. The authors are indebted to Centro de Supercomputación of Galicia (CESGA) for providing the computer facilities.

Notes and references

1. R. M. Harrison, D. R. H. Laxen, *Lead Pollution*, Chapman and Hall, London, 1981.
2. G. F. Nordberg, *BioMetals*, 2004, **17**, 485–489.
3. H. Sigel, C. P. Da Costa and R. B. Martin, *Coord. Chem. Rev.*, 2001, **219–221**, 435–461.
4. H. Sigel, B. E. Fischer and E. Farkas, *Inorg. Chem.*, 1983, **22**, 925–934.
5. H. A. Tajimir-Riahi, M. Langlais and R. Savoie, *Nucleic Acids Res.*, 1988, **16**, 751–762.
6. (*a*) G. Kazantis, in *Poisoning, Diagnosis and Treatment* ed. J. A. Vale and T. J. Meredith, Update Books, London, 1981, pp. 171–175; (*b*) D. Baltrop, in *Poisoning, Diagnosis and Treatment* ed. J. A. Vale and T. J. Meredith, Update Books, London, 1981, pp. 178–185.
7. C. P. Da Costa and H. Rigel, *Inorg. Chem.*, 2000, **39**, 5985–5993.
8. R. B. Martin, *Inorg. Chim. Acta*, 1998, **283**, 30–36.
9. J. S. Magyar, T.-C. Weng, Ch. M. Stern, D. F. Dye, B. W. Rous, J. C. Payne, M. A. Bridgewater, B. Mijovilovich, G. Parkin, J. M. Zaleski, J. E. Penner-Hahn and H. A. Godwin, *J. Am. Chem. Soc.*, 2005, **127**, 9495–9505.

10. J. M. Christensen, J. Kristiansen, in *Handbook of Metals in Clinical and Analytical Chemistry*, ed. H. G. Seiler, A. Sigel and H. Sigel, Marcel Dekker, New York, 1994, pp. 425–440.

11. R. A. Goyer, in *Handbook on Toxicity of Inorganic Compounds* ed. H. G. Seiler, A. Sigel and H. Sigel, Marcel Dekker, New York, 1988, pp. 359–382.

12. B. P. Lanphear, R. Hornung, J. Khoury, K. Yolton, P. Baghurst, D. C. Bellinger, R. L. Canfield, K. N. Dietrich, R. Bornschein, T. Greene, S. J. Rothenberg, H. L. Needleman, L. Schnaas, G. Wasserman, J. Graziano and R. Roberts, *Environ. Health Perspect.*, 2005, **113**, 894–899.

13. C. Castellino, P. Caselino, N. Sannolo, *Inorganic Lead Exposure: Metabolism and Intoxication*, Lewis, Boca Raton, FL, USA, 1994.

14. F. M. R. Bulmer, H. E. Rothwell and E. R. Frankish, *Can. Public Health J.*, 1938, **29**, 19–26.

15. A. T. Yordanov and D. M. Roundhill, *Coord. Chem. Rev.*, 1998, **170**, 93–124.

16. L. Shimoni-Livny, J. P. Glusker and C. W. Bock, *Inorg. Chem.*, 1998, **37**, 1853–1867.

17. A. Pellissier, Y. Bretonniere, N. Chatterton, J. Pecaut, P. Delangle and M. Mazzanti, *Inorg. Chem.*, 2007, **46**, 3714–3725.

18. R. D. Hancock, A. S. de Sousa, G. B. Walton and J. H. Reibenspies, *Inorg. Chem.*, 2007, **46**, 4749–4757.

19. C. Platas-Iglesias, M. Mato-Iglesias, K. Djanashvili, R. N. Muller, L. Vander Elst, J. A. Peters, A. de Blas and T. Rodríguez-Blas,*Chem.–Eur. J.*, 2004, **10**, 3579–3590.

20. E. J. T. Chrystal, L. Couper and D. J. Robins, *Tetrahedron*, 1995, **51**, 10241–10252.

21. P. Caravan, S. L. Rettig and C. Orvig, *Inorg. Chem.*, 1997, **36**, 1306–1315.

22. (*a*) V. Rodriguez, J. M. Gutierrez-Zorrilla, P. Vitoria, A. Luque, P. Roma and M. Martinez-Ripoll, *Inorg. Chim. Acta*, 1999, **290**, 57–63; (*b*) R. Meier, M. Molinier, C. Anson, A. K. Powell, B. Kallies and R. van Eldik, *Dalton Trans.*, 2006, 5506–5514.

23. C. M. Armstrong, P. V. Bernhardt, P. Chin and D. R. Richardson, *Eur. J. Inorg. Chem.*, 2003, 1145–1156.

24. (*a*) K. A. Jensen, *Inorg. Chem.*, 1970, **9**, 1–5; (*b*) C. Platas, F. Avecilla, A. de Blas, T. Rodríguez-Blas, R. Bastida, A. Macías, A. Rodríguez and H. Adams, *J. Chem. Soc., Dalton Trans.*, 2001, 1699–1705.

25. M. Mato-Iglesias, E. Balogh, C. Platas-Iglesias, É. Toth, A. de Blas and T. Rodríguez-Blas, *Dalton Trans.*, 2006, 5404–5415.

26. R. K. Harris, *Nuclear Magnetic Resonance Spectroscopy: A Physicochemical View*, Pitman, London, 1983.

27. (*a*) C. Platas-Iglesias, D. Esteban-Gómez, T. Enríquez-Pérez, F. Avecilla, A. de Blas and T. Rodríguez-Blas, *Inorg. Chem.*, 2005, **44**, 2224–2233; (*b*) D. Esteban-Gómez, C. Platas-Iglesias, T. Enríquez-Pérez, F. Avecilla, A. de Blas and T. Rodríguez-Blas, *Inorg. Chem.*, 2006, **45**, 5407–5416.

28. (*a*) D. Esteban-Gómez, C. Platas-Iglesias, F. Avecilla, A. de Blas and T. Rodríguez-Blas, *Eur. J. Inorg. Chem.*, 2007, 1635–1643; (*b*) M. Regueiro-Figueroa, D. Esteban-Gómez, C. Platas-Iglesias, A. de Blas and T. Rodríguez-Blas, *Eur. J. Inorg. Chem.*, 2007, 2198–2207.

29. T. Yamaki and K. Nobusada, *J. Phys. Chem. A*, 2003, **107**, 2351–2358.

30. M. Di Vaira, F. Mani, S. S. Constantini, P. Stoppioni and A. Vacca, *Eur. J. Inorg. Chem.*, 2003, 3185–3192.

31. G. Akibo-Betts, P. E. Barran, L. Puskar, B. Duncombe, H. Cox and A. J. Stace, *J. Am. Chem. Soc.*, 2002, **124**, 9257–9264.

32. R. D. Hancock and A. E. Martell, *Chem. Rev.*, 1989, **89**, 1875–1914.

33. R. G. Lacoste, G. V. Christoffers and A. E. Martell, *J. Am. Chem. Soc.*, 1965, **87**, 2385–2388.

34. A. E. Martell, R. J. Motekaitis, R. M. Smith, *NIST Critically selected stability constants of metal complexes database*, National Institute of Standards and Technology, Standard Reference Data Program, Gaithersburg, MD, USA, version 8.0 for windows, 2004.

35. Y. Sun, A. E. Martell, J. H. Reibenspies, D. E. Reichert and M. J. Welch, *Inorg. Chem.*, 2000, **39**, 1480–1486.

36. (*a*) R. W. Peters, *J. Hazard. Mater.*, 1999, **66**, 151–210.

37. E. Balogh, M. Mato-Iglesias, C. Platas-Iglesias, É. Tóth, K. Djanashvili, J. A. Peters, A. de Blas and T. Rodríguez-Blas, *Inorg. Chem.*, 2006, **45**, 8719–8728.

38. W. C. Wolsey, *J. Chem. Educ.*, 1973, **50**, A335.

39. P. Gans, A. Sabatini and A. Vacca, *Talanta*, 1996, **43**, 1739–1753.

40. WinGX 1.70.01 An integrated system of Windows programs for the solution, refinement and analysis of single crystal X-ray diffraction data, L. J. Farrugia, *J. Appl. Crystallogr.*, 1999, **32**, 837–838.

41. G. M. Sheldrick, *Acta Crystallogr., Sect. A: Found. Crystallogr.*, 2008, **64**, 112–122.

42. P. T. Beurskens, G. Beurskens, R. de Gelder, S. Garcia-Granda, R. O. Gould, R. Israel and Jan M. M. Smits, *The DIRDIF-99 program system*, Crystallography Laboratory, University of Nijmegen, The Netherlands, 1998.

43. A. Altomare, G. Cascarano, C. Giacovazzo and A. Guagliardi, *J. Appl. Crystallogr.*, 1993, **26**, 343–350.

44. G. M. Sheldrick, *SADABS, Program for area detector adsorption correction*, Institute for Inorganic Chemistry, University of Göttingen, Germany, 1996.

45. A. L. Spek, *Acta Crystallogr., Sect. A: Found. Crystallogr.*, 1990, **46**, C34.

46. A. D. Becke, *J. Chem. Phys.*, 1993, **98**, 5648–5652.

47. C. Lee, W. Yang and R. G. Parr, *Phys. Rev. B: Condens. Matter Mater. Phys.*, 1988, **37**, 785–789.

48. P. J. Hay and W. R. Wadt, *J. Chem. Phys.*, 1985, **82**, 270–283.

49. A description of the basis sets and theory level used in this work can be found in: J. B. Foresman, A. E. Frisch, *Exploring Chemistry with Electronic Structure Methods*, Gaussian Inc., Pittsburgh, PA, 2nd edn, 1996.

50. V. Barone and M. Cossi, *J. Phys. Chem. A*, 1998, **102**, 1995–2001.

51. E. D. Glendening, A. E. Reed, J. E. Carpenter, F. Weinhold, NBO version 3.1.

52. A. E. Reed, L. A. Curtiss and F. Weinhold, *Chem. Rev.*, 1988, **88**, 899–926.

53. M. J. Frisch, G. W. Trucks, H. B. Schlegel, G. E. Scuseria, M. A. Robb, J. R. Cheeseman, J. A. Montgomery, Jr., T. Vreven, K. N. Kudin, J. C. Burant, J. M. Millam, S. S. Iyengar, J. Tomasi, V. Barone, B. Mennucci, M. Cossi, G. Scalmani, N. Rega, G. A. Petersson, H. Nakatsuji, M. Hada, M. Ehara, K. Toyota, R. Fukuda, J. Hasegawa, M. Ishida, T. Nakajima, Y. Honda, O. Kitao, H. Nakai, M. Klene, X. Li, J. E. Knox, H. P. Hratchian, J. B. Cross, V. Bakken, C. Adamo, J. Jaramillo, R. Gomperts, R. E. Stratmann, O. Yazyev, A. J. Austin, R. Cammi, C. Pomelli, J. W. Ochterski, P. Y. Ayala, K. Morokuma, G. A. Voth, P. Salvador, J. J. Dannenberg, V. G. Zakrzewski, S. Dapprich, A. D. Daniels, M. C. Strain, O. Farkas, D. K. Malick, A. D. Rabuck, K. Raghavachari, J. B. Foresman, J. V. Ortiz, Q. Cui, A. G. Baboul, S. Clifford, J. Cioslowski, B. B. Stefanov, G. Liu, A. Liashenko, P. Piskorz, I. Komaromi, R. L. Martin, D. J. Fox, T. Keith, M. A. Al-Laham, C. Y. Peng, A. Nanayakkara, M. Challacombe, P. M. W. Gill, B. Johnson, W. Chen, M. W. Wong, C. Gonzalez, and J. A. Pople, *GAUSSIAN 03 (Revision C.01)*, Gaussian, Inc., Wallingford, CT, 2004.

† Electronic supplementary information (ESI) available: Fig. S1 showing ^{1}H NMR spectra of ligand bcpc and its Zn(II), Cd(II) and Pb(II) complexes and *in vacuo* optimized Cartesian coordinates (Å) for the [Pb(L)] systems (L = bcpe or bcpc). CCDC reference numbers 689091–689095. For ESI and crystallographic data in CIF or other electronic format see DOI: 10.1039/b808631a.